Climate Dynamics (1994) 9:303–319

Climate Dynamics

Decadal atmosphere-ocean variations in the Pacific

Kevin E Trenberth, James W Hurrell

National Center for Atmospheric Research, P. O. Box 3000, Boulder, CO 80307, USA

Received: 24 November 1992/Accepted: 5 April 1993

Abstract. Considerable evidence has emerged of a substantial decade-long change in the north Pacific atmosphere and ocean lasting from about 1976 to 1988. Observed significant changes in the atmospheric circulation throughout the troposphere revealed a deeper and eastward shifted Aleutian low pressure system in the winter half year which advected warmer and moister air along the west coast of North America and into Alaska and colder air over the north Pacific. Consequently, there were increases in temperatures and sea surface temperatures (SSTs) along the west coast of North America and Alaska but decreases in SSTs over the central north Pacific, as well as changes in coastal rainfall and streamflow, and decreases in sea ice in the Bering Sea. Associated changes occurred in the surface wind stress, and, by inference, in the Sverdrup transport in the north Pacific Ocean. Changes in the monthly mean flow were accompanied by a southward shift in the storm tracks and associated synoptic eddy activity and in the surface ocean sensible and latent heat fluxes. In addition to the changes in the physical environment, the deeper Aleutian low increased the nutrient supply as seen through increases in total chlorophyll in the water column, phytoplankton and zooplankton. These changes, along with the altered ocean currents and temperatures, changed the migration patterns and increased the stock of many fish species. A north Pacific (NP) index is defined to measure the decadal variations, and the temporal variability of the index is explored on daily, annual, interannual and decadal time scales. The dominant atmosphere-ocean relation in the north Pacific is one where atmospheric changes lead SSTs by one to two months. However, strong ties are revealed with events in the tropical Pacific, with changes in tropical Pacific SSTs leading SSTs in the north Pacific by three months. Changes in the storm tracks in the north Pacific help to reinforce and maintain the anomalous circulation in the upper troposphere. A hypothesis is put forward outlining the tropical and extratropical realtionships which stresses the role of tropical forcing but with important feedbacks in the extratropics that serve to emphasize the decadal relative to interannual time scales. The Pacific decadal timescale variations are linked to recent changes in the frequency and intensity of El Niño versus La Niña events but whether climate change associated with "global warming" is a factor is an open question.

The National Center for Atmospheric Research is sponsored by the National Science Foundation

1 Introduction

It has often been stated that the atmosphere has a very short memory while the ocean has enormous thermal inertia so that it is the ocean that provides the important memory for climate variations. In fact, however, it is the collaborative interaction between the atmosphere and the ocean and other parts of the climate system that gives rise to the important climate variations. In this study, we document recent important variations on decadal time scales involving both the atmosphere and the ocean in the north Pacific and we explore the links to other parts of the globe. The variations described emphasize the very large scales that are apparently set by the scales of the atmospheric planetary-scale waves.

Climate variations over the north Pacific and teleconnections downstream across North America have long been of interest and have been particularly highlighted by the work of Namias (1959, 1963, 1969). Recently, considerable evidence has emerged of a decade-long change in the north Pacific atmosphere and ocean that began about 1976. Changes in the atmospheric circulation throughout the troposphere at this time have been documented by Trenberth (1990, see Fig. 1) and Nitta and Yamada (1989) for the winter half year. These changes were associated with changes in the surface wind stress and, by inference, in the Sverdrup transport in the north Pacific Ocean (Trenberth 1991a;

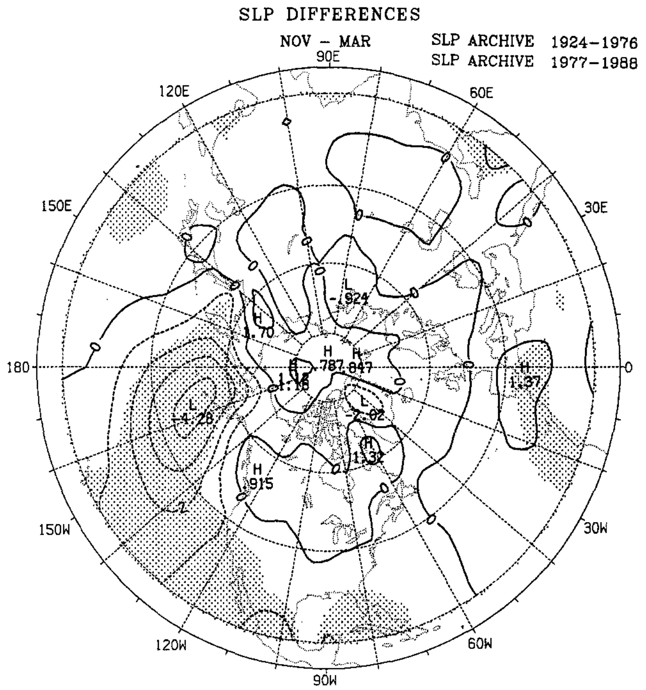

Fig. 1. The difference in mean sea level pressures from 1977 to 1988 for November through March versus 1924 to 1976 (mb). *Stippling* indicates statistical significance at 5%. From Trenberth (1990)

Trenberth et al. 1989) that have been directly measured in the Gulf of Alaska (Royer 1989). Bakun (1990) has noted changes in the longshore wind stress off California that are probably related. Changes in the monthly mean flow also imply changes in the storm tracks and associated synoptic eddy activity (e.g., Rogers and Raphael 1992; Lau 1988) and in the surface ocean sensible and latent heat fluxes (Cayan 1992). The circulation changes were accompanied by changes in heat and moisture advection by the quasistationary flow (e.g., Rogers and Raphael 1992), so that there were substantial changes in the temperatures along the west coast of North America and in sea surface temperatures (SSTs) over the north Pacific (Trenberth 1990; Salmon 1992), as well as in coastal rainfall and streamflow (Cayan and Peterson 1989), and sea ice in the Bering Sea (Manak and Mysak 1987). Also accompanying the changes in the Pacific were higher incidences of cold outbreaks across the plains of North America ultimately leading to major freezes affecting the Florida citrus crop (Rogers and Rohli 1991; Downton and Miller 1993).

In addition to the changes in the physical environment, Venrick et al. (1987) observed associated large changes in the epipelagic ecosystem in the North Pacific, with increases in total chlorophyll in the water column, and thus in phytoplankton. McFarlane and Beamish (1992) link these changes to the sustantial increases reported in the dominant zooplankton, calanoid copepods, after 1976. Mysak (1986) earlier noted that the changes in ocean currents and temperatures had altered the migration patterns of fish, in particular tuna and salmon, in the northeast Pacific; see also Hamilton (1987). Ebbesmeyer et al. (1991) found that the "step in Pacific climate" in 1976 had a profound effect on forty environmental variables. They contrasted the periods 1968–1975 with 1977–1984 and noted that in addition to these parameters, climate-related changes were found in the behavior of geese, salmon, and crabs in the northeast Pacific, and mollusk abundance, salinity and water temperature in Puget Sound. McFarlane and Beamish (1992) proposed that the cooling of the central north Pacific Ocean increased nutrient supply to the surface waters thereby improving primary productivity, to the benefit of many fish species; in particular they document substantial increases in sablefish. They further link the years of good recruitment to a more intense Aleutian low in winter.

The change in 1976 is but one of several large changes that have occurred in the north Pacific. As noted, Namias has documented decadal-scale variations in the past, with coherent signals in the atmospheric circulation and in the sea surface temperatures, and with teleconnections downstream across North America; see also Dickson and Namias (1976), Douglas et al. (1982) and Namias et al. (1988). The fairly sluggish response of the mid-latitude ocean to changes in the ocean forcing through the surface momentum and heat fluxes effectively serves as a low-pass filter and emphasizes the longer time scales. More recent studies throw further light on these aspects and on the physical links between the atmosphere and ocean in the north Pacific, and will be discussed later. New evidence has also emerged on the telectonnections downstream across North America, associated, in particular, with the PNA (Pacific-North American) teleconnection pattern.

Possible causes of the changes were discussed by Trenberth (1990) who noted the close link between north Pacific changes on the decadal time scale with those in the tropical Pacific and Indian Ocean, and the changes in frequency and intensity of El Niño versus La Niña events. This expanded on the similar link noted during El Niño events by Bjerknes (1969). These aspects will be pursued and quantified further later. Yamagata and Masumoto (1992) have suggested, however, that the decadal time-scale variations may also involve the Asian monsoon system.

The time series in Trenberth (1990) ceased after the northern winter of 1987–88 and it is of considerable interest to see what the subsequent evolution has been. Accordingly, in this study we update the time series and carry out some more comprehensive correlation analyses with surface temperature and SST analyses, and examine further the links with the tropical Pacific and the Southern Oscillation. It is also of interest to examine the time scales of the main circulation anomaly patterns contributing to the decadal variation and the associated changes in storm tracks and feedbacks of the anomalous transient eddy fluxes of heat and vorticity on the mean flow anomalies.

2 North Pacific large-scale observed trends

Most presentations of climate change focus on the surface variables of importance to man, in particular temperature and precipitation. However, to understand why the changes occur the way they do, it is essential to consider the atmospheric dynamics as well as the local physical processes operating to induce change. The atmospheric circulation forms the main link between regional changes in wind, temperatures, precipitation and other climatic variables. Physical and dynamical consistency between changes of several climate variables can add confidence to results for a single variable which might otherwise be compromised by measurements, data coverage, or analysis uncertainties.

In the north Pacific, a close association between SST anomalies and the atmospheric circulation has been well recognized by Namias (1959, 1963, 1969), Namias et al. (1988), Davis (1976, 1978), Lanzante (1984), and Wallace et al. (1990). Changes in surface temperatures arise from changes in temperature and moisture advection over the oceans by anomalous winds and through the associated changes in surface fluxes and vertical mixing within the ocean. Anomalous northerly winds over the ocean are typically not only cold but also dry, so that large increases in surface fluxes of both sensible and latent heat can be expected into the atmosphere, thereby cooling the ocean. Convection and mechanical mixing in the ocean can spread those influences through considerable depth and may also entrain water from below the thermocline, prolonging the lifetime of the anomalies (e.g., Frankignoul 1985).

2.1 *Circulation indices*

In the SSTs, a very distinctive pattern (cf. Fig. 9) emerges as the dominant mode of an empirical orthogonal function (EOF) analysis (Davis 1976; Lau and Nath 1990) that is linked with a preferred mode of variability in winter in the Northern Hemisphere (NH) and is similar to the PNA teleconnection pattern of Wallace and Gutzler (1981). The PNA consists of four centers of action in the mid-tropospheric height field, near Hawaii and along the west coast of North America of one sign, and of opposite sign over the north Pacific and southeast United States. Wallace and Gutzler (1981) defined a PNA index using single point values of 500 mb monthly mean geopotential height at each of the centers:

$$PNA = \tfrac{1}{4}\,[z^*(20°\mathrm{N}, 160°\mathrm{W}) - z^*(45°\mathrm{N}, 165°\mathrm{W}) + z^*(55°\mathrm{N}, 115°\mathrm{W}) - z^*(30°\mathrm{N}, 85°\mathrm{W})] \quad (1)$$

where z^* is the normalized 500 mb geopotential height anomaly, i.e., the height departure from the mean divided by the standard deviation.

Although this has proven to be a useful index, it does not appropriately weight the four centers of the PNA, in which the north Pacific center is by far the most prominent in the height field. In addition, by using values only at the centers rather than defining the whole pattern over the grid, the index is sensitive to errors in the analyses. Leathers and Palecki (1992) examine the PNA index and the four point values and find an abrupt change in 1957 in the southeast United States point. The change coincides with the transition from 0300 and 1500 to 0000 and 1200 UTC rawinsonde soundings. Although they conclude that the change is real, we have carried out a more detailed analysis of related variables which has convinced us that part of the change is spurious[1], and this leads to spurious trends in the PNA index. In addition, a change in the time scale from monthly means to daily analyses, for instance, introduces much more structure in the field, so that an index based on only point values will be heavily aliased.

Northern Hemispheric analyses of the atmospheric circulation above the surface are confined to after 1947, but a long series of charts of sea level pressure variations, beginning in 1899, are available. An evaluation (Trenberth and Paolino 1980) shows them to be most reliable after 1924, and as in Trenberth (1990), we therefore use monthly mean sea level pressures after this date to examine the changes in circulation. Wallace and Gutzler (1981) show that the surface signature of the PNA is mostly confined to the Pacific. We therefore choose a much more robust but simple measure of the circulation in the north Pacific as the area-weighted mean sea level pressure over the region 30 to 65° N, 160° E to 140° W. We refer to this as the NP index (for north Pacific). This is slightly smaller than the area used in Trenberth (1990) but better corresponds to the area participating in the decadal time scale variations (see Fig. 1). The correlation of the NP index with the PNA index defined in (1) for 5-month averages (November–March) is −0.91 for 1947–1991. As well as being an index of the PNA teleconnection pattern, the NP time series depicts changes in the intensity of the the Aleutian low in winter.

2.2 *Time scales of the NP index*

Figure 2 shows the NP index for all months of the year from 1924 through 1992. This reveals the total value of the index, and thus includes the mean annual cycle, for three-month (seasonal) means that have been smoothed in time using a low pass filter [with weights (1, 4, 8, 10, 8, 4, 1)/36] which emphasizes the interdecadal fluctuations. Figure 3 shows the anomalies: firstly, the individual monthly values (with the mean annual cycle removed) are rather noisy and month-to-month variations are prominent; and secondly, the anomalies from Fig. 2 as a smoothed version of the

[1] Leathers and Palecki consider the surface temperatures in the southeast United States and show that a change also occurred in those records in 1957. They presented time series for 1950 to 1965. However, longer series to 1990 reveal that while the surface temperatures return to values similar to those prior to 1957, the 500 mb heights do not

first panel reveal the most persistent anomalies. The figures emphasize that the period November through March corresponds to the winter time regime, with low pressures in the Pacific, while for the rest of the year, the Pacific tends to be dominated more by the subtropical anticyclone. Also, the main variability occurs only in the November through March months. Standard deviations of the monthly anomaly time series range from about 1 mb in the summer months to >4.5 mb in January and February. Values exceed 2.8 mb only from November through March.

The variability from one month to the next in the same winter season arises from transient atmospheric variations that are poorly sampled using monthly data. To explore this aspect in more detail, the NP index has also been created from the area average of 1000 mb geopotential height using 12 hourly European Centre for Medium Range Weather Forecasts (ECMWF) global analyses from 1980 through 1991. Figure 4 shows the daily mean and standard deviations over the 12 years along with a smoothed mean annual cycle. As in Fig. 2 it reveals the lower NP values in the winter half year and the larger interannual variability from November through March. It also reveals an interesting dip in the annual cycle about the beginning of June

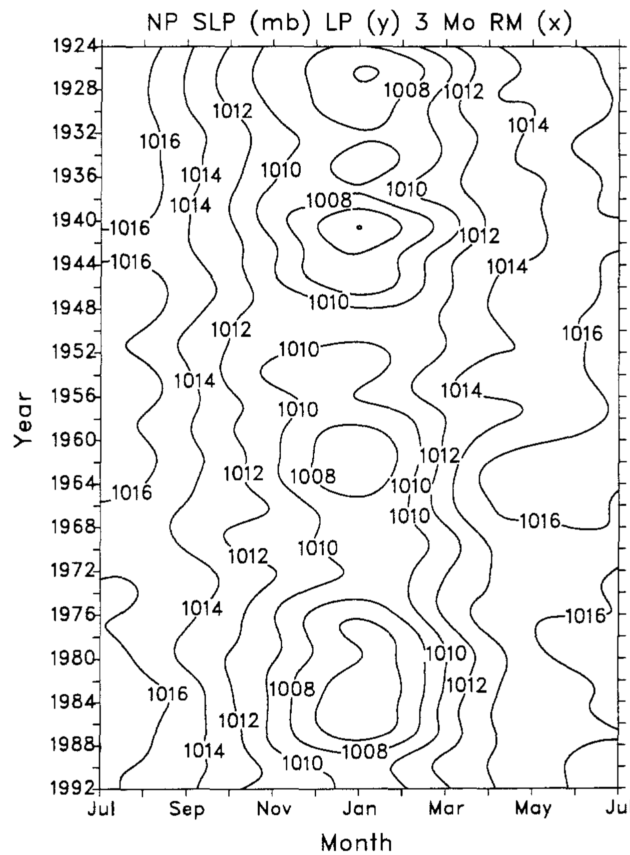

Fig. 2. Time series of NP, the mean north Pacific sea level pressures averaged over 30 to 65°N, 160°E to 140°W as a function of month and time. Shown is the total three-monthly mean values smoothed with a low pass filter with seven weights (1, 4, 8, 10, 8, 4, 1)/36 across years to emphasize the decadal time scales in mb

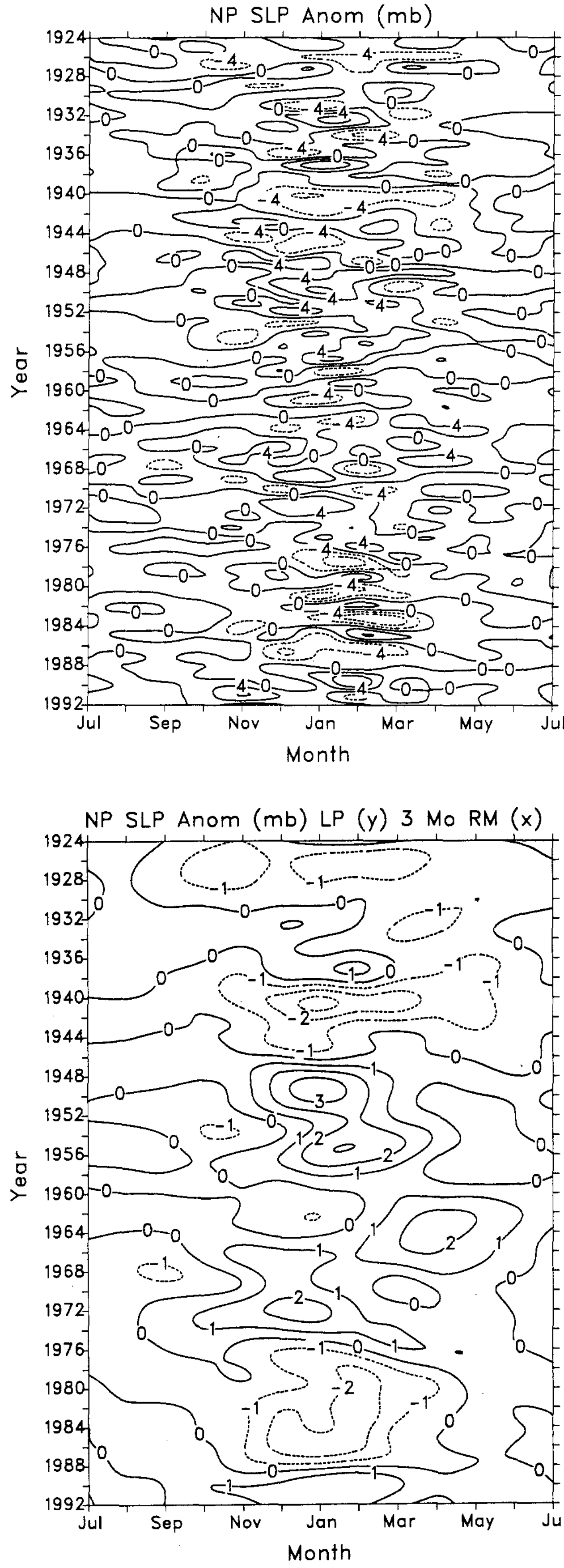

Fig. 3. As in Fig. 2 but *top* monthly mean anomalies in mb, and *bottom* seasonal (three month) mean anomalies smoothed with the low pass filter in mb

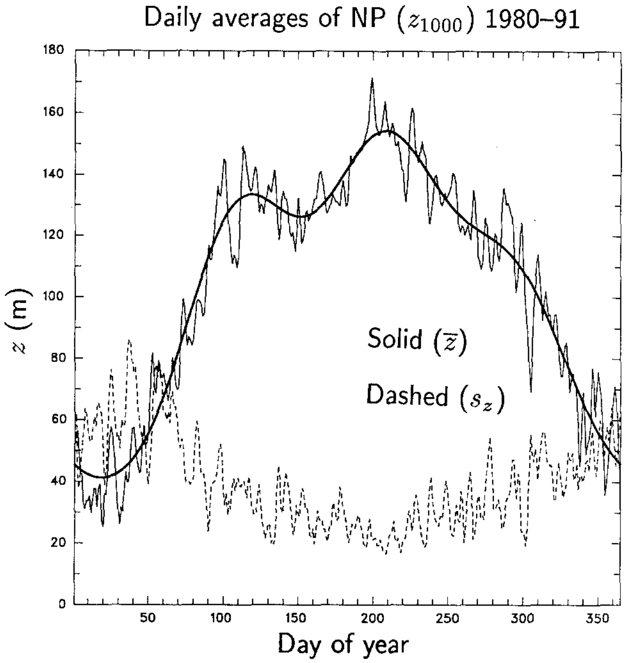

Fig. 4. Daily averages (*thin solid*) and standard deviations (*dashed*) of the NP index in the form of the 1000 mb height as a function of day of the year. Averages are over the twelve years 1980 to 1991. The *heavy solid curve* shows the fit of the first four harmonics to the mean annual cycle

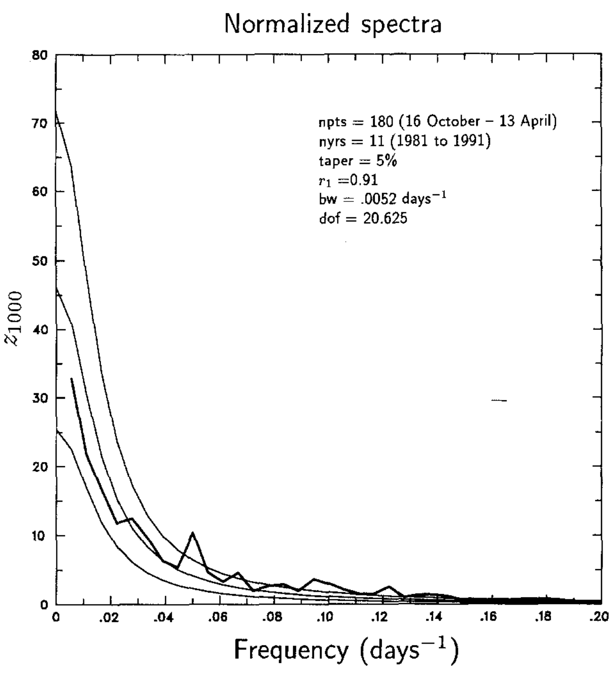

Fig. 5. Power spectrum of the 1000 mb NP index anomalies (departures from the smoothed mean annual cycle in Fig. 3) averaged over the 11 winter half years from 16 October to 13 April, 1980–81 to 1990–91. A taper of 5% of the values at each end was applied. Also shown is the corresponding red noise spectrum with the same lag one autocorrelation coefficient (0.91) and the 5 and 95% confidence limits. Only the spectrum for frequencies from 0 to 0.2 days^{-1} is shown, at higher frequencies, the power is close to zero

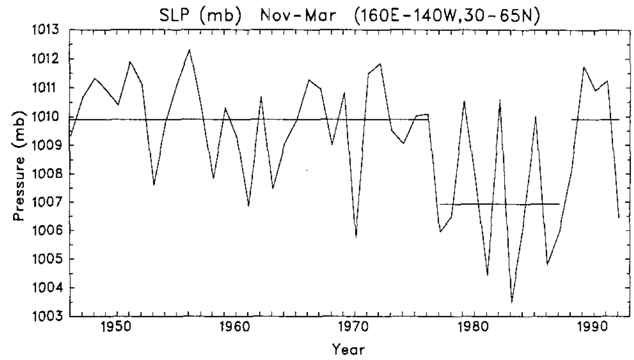

Fig. 6. Time series of mean north Pacific sea level pressures averaged over 30 to 65°N, 160°E to 140°W for the months November through March. Means for 1946–1976 plus 1989–1992 and 1977–1988 are indicated (where 1988 refers to the 1987–88 winter)

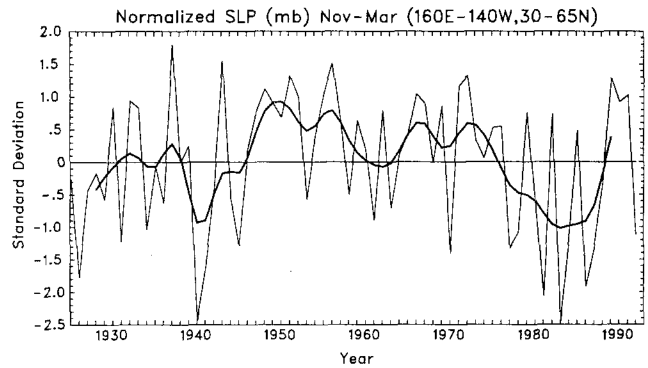

Fig. 7. Time series of mean north Pacific sea level pressures for November through March, as in Fig. 3, but beginning in 1925 and smoothed with the low pass filter

(day 150) that interrupts the otherwise smooth tendency towards high NP values in the northern summer.

Because the removal of the mean annual cycle still leaves an annual cycle in variance, a power spectrum is computed from daily NP values for the winter half year (Fig. 5). This reveals almost no power at periods less than a week (not shown) and a fairly red spectrum (autocorrelation of daily values 0.91), but with one especially notable and highly significant spectral peak at 20 days period. This stems from well documented 20-day period westward propagating planetary-scale waves (Kushnir 1987; Branstator 1987; Madden and Speth 1989). Monthly means are far from optimal when strong 20-day period fluctuations are present, but averaging over the five winter months removes much of this kind of noise.

Accordingly, Figs. 6 and 7 show the NP time series for the five month winter time average. In Fig. 6 the 1946–1992 time series is broken up to emphasize the regime from November 1976 to March 1988, while in Fig. 7 the time series from 1925 is shown with the low pass curve to reveal, without the arbitrariness of deciding on a start and end for the regime, just how unusual the 1976 to 1988 period is; the only previous time that comparable values occurred was for the much shorter

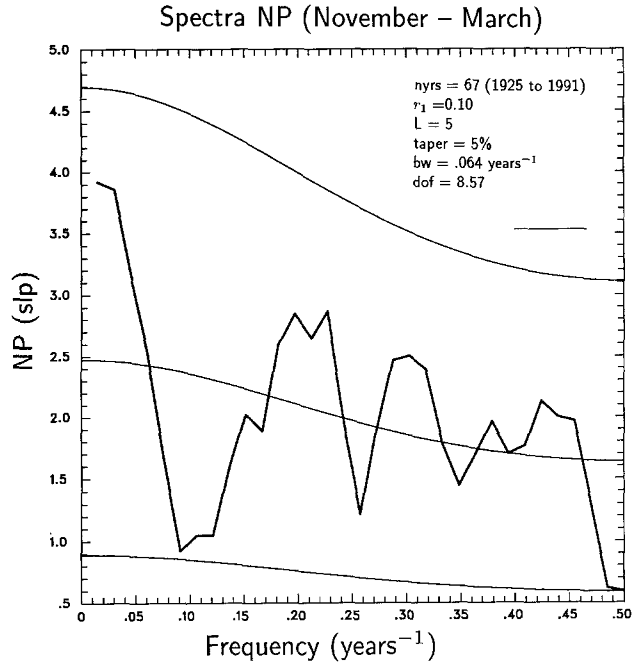

Fig. 8. Power spectrum of the NP index for November through March averages for the 67 years from 1924–25 to 1990–91. A taper of 5% of the values at each end was applied and the spectral estimates were averaged over 5 values. Also shown is the corresponding red noise spectrum with the same lag one autocorrelation coefficient (0.91) and the 5 and 95% confidence limits

interval from 1940 to 1941. There is, nevertheless, considerable interannual variability present within the regime.

In the Aleutian low for November through March from 1976–77 to 1987–88, pressures were lower by 3.0 mb averaged over the NP area of the north Pacific (Fig. 6). Lower pressures were present individually in all five winter months, and are highly statistically significant (Fig. 1). No such change is present in any of the other months of the year (Fig. 3). The winter time changes correspond to the center of the low farther east and deeper on average by 4.3 mb for the five winter months, and deeper by 7 to 9 mb in January (Trenberth 1991a; see also Fig. 1). A spectrum of the five-month winter mean NP index is shown in Fig. 8 for the 67 years 1925 to 1991. Using a red noise null hypothesis, no significant spectral peaks emerge. However, the spectra do reveal several features of interest. The first is enhanced variance in several spectral peaks between about 2 and 6 year periodicities which are believed to be associated with the El Niño – Southern Oscillation (ENSO) phenomenon. The second is a deficit in power at 7 to 12 year periods, and the third is the enhanced power in a broad spectral peak featuring periods of >20 years or so. This is the interdecadal variability[2].

Large-scale changes in both atmospheric and oceanic fields over the north Pacific have been previously noted by Douglas et al. (1982) who contrasted the 1969–1980 period with 1947–1966 and found a correspondence between the pattern of lower SSTs to strengthened northerly wind and/or lower 700 mb heights. Our time series (Figs. 6 and 7), however, indicate that a more coherent picture emerges if the different regime is considered to have begun in late 1976.

A climatology for surface wind stress based on 1980 to 1986 (Trenberth et al. 1989) revealed changes in the north Pacific from the Hellerman and Rosenstein (1983) climatology, based on ship data prior to 1977, that help confirm the reality of the sea level pressure changes (Trenberth 1991a), and so do analyses with independent data sets (Nitta and Yamada 1989). Moreover, the associated changes in the curl of the wind stress and the corresponding Sverdrup transport in the ocean (Trenberth et al. 1989) over such a long period imply significant changes in the North Pacific Ocean currents (see Sekine 1988).

2.3 *Observed relationships*

The corresponding changes in surface temperatures are shown in Fig. 9. The surface temperatures are taken from the updated Intergovernmental Panel on Climate Change (IPCC) data set (IPCC 1900, 1992) which consists of land surface data from the University of East Anglia (Jones 1988) blended with sea surface temperature data from the United Kingdom Meteorological Office (Bottomley et al. 1990); see also Trenberth et al. (1992). Shown are both the surface temperature anomalies, expressed as departures from the 1951–80 means, for both the whole year and the five winter months November–March averaged over the 1977–1988 period. The temperature anomalies are strongly regional and of both positive and negative signs. The twelve year period features very large north Pacific basin temperature anomalies, with warming of over 1.5° C in Alaska and cooling of >0.5° C in the central north Pacific. The pattern in Fig. 9 over the north Pacific is very similar to the first EOF of SSTs (Davis 1976; Lau and Nath 1990). The annual mean anomaly clearly arises from the winter time atmospheric anomaly but over the north Pacific there is sufficient persistence throughout the year that little difference exists between the annual and five-month means. The winter time pattern also reveals below normal temperatures over the southeastern part of the United States, illustrating the PNA teleconnection. These mean conditions provide a background in which cold outbreaks from the north into the United States are more likely to penetrate to the Gulf Coast, and this results in a higher than usual incidence of major freezes affecting the Florida citrus crop after 1977 (Rogers and Rohli 1991; Downton and Miller 1993).

The most compelling argument that the changes in sea level pressure are real is the physical consistency with the very large regional Pacific temperature anomalies for 1977–88 in Fig. 9. The warming over Alaska and along the west coast of North America, in addition

[2] Note there is often confusion over time scale and period. For a regime, the time duration (or time scale) is half the period

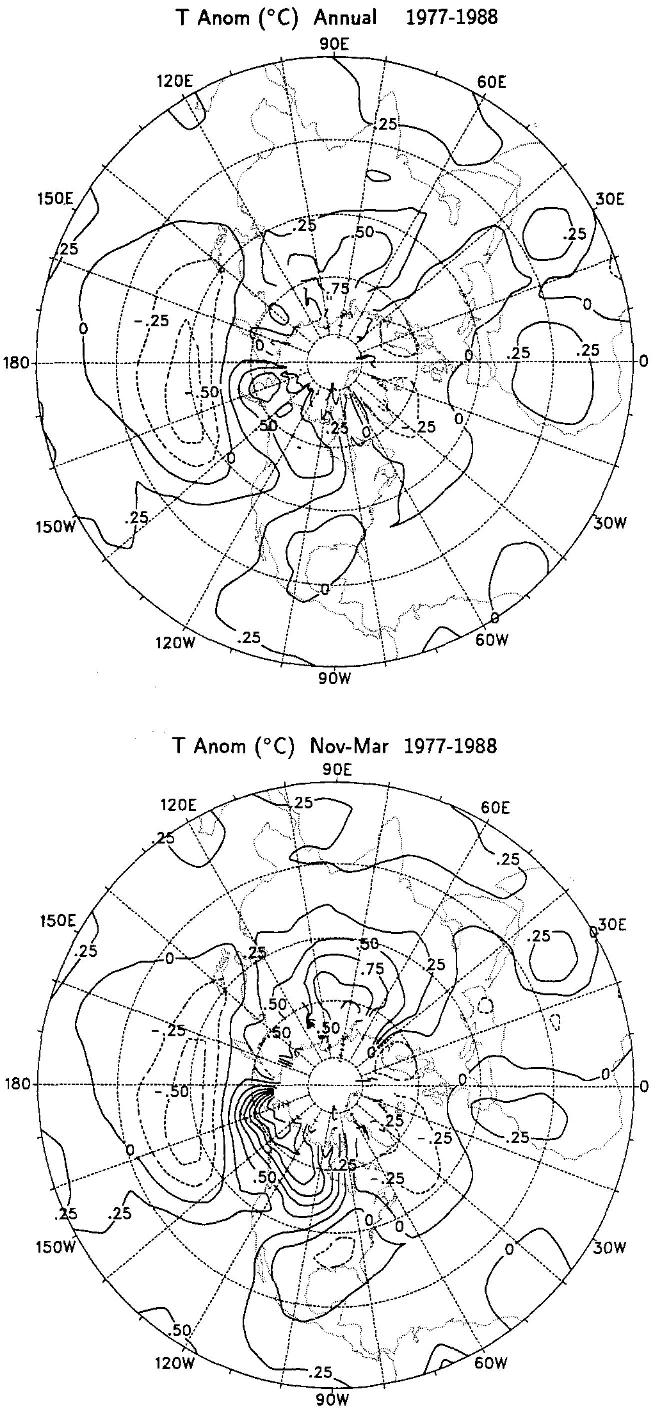

Fig. 9. Twelve year (1977–1988) average surface temperature or sea surface temperature anomalies as departures from the 1951–1980 mean. *Contours* every 0.25° C. Shown are the annual mean anomalies and the anomalies for the 5 winter months (November to March). Negative values are *dashed*

to the cooling in the central and western north Pacific, would be expected with a stronger Aleutian low from considerations of thermal advection (Rogers and Raphael 1992) and increased ocean mixing and changes in the surface fluxes (Cayan 1992; Alexander 1992a, b). The increased southward gradient flow in the eastern north Pacific, revealed by the pressure pattern in Fig. 1, would bring warmer and moister air into Alaska and along the west coast of North America, while anomalous northerly winds would give rise to colder than normal conditions in the central and western north Pacific. Lower SSTs result from large sensible and latent heat fluxes into the atmosphere combined with increased mixing in the ocean (Cayan 1992). Cayan and Peterson (1989) found that increased streamflow in the Alaskan coastal region of the northern Gulf of Alaska occurs from increased coastal rainfall associated with a deepened Aleutian low and changes in the PNA.

To further show the nature of the surface temperature changes associated with the NP index, Fig. 10 shows the correlations for the five-month average November–March from 1935 to 1990 along with the corresponding departure pattern in degrees C associated with a unit standard deviation departure of the NP index. Across the north Pacific and North American regions, these patterns show that the anomaly featured in Fig. 9 is consistent with the whole record: below normal NP values are associated with below normal temperatures over the north Pacific and southeast United States and above normal surface temperatures along the west coast, extending throughout Alaska and across most of Canada. We have also investigated these relationships as a function of various lags. To decide objectively on how much variance is explained by the correlations across an area, we have averaged the correlation coefficient squared for the region 140°E to 60°W, 30 to 65°N. Largest surface temperature variance explained by the NP index for this region occurs with NP leading by 1 to 2 months (r^2 values with NP leading by 3, 2, 1 and 0 months are 0.15, 0.19, 0.20 and 0.16). The pattern is similar to that at zero lag but the correlation coefficients increase in magnitude by about 0.1 (to >0.6 over the North Pacific, and to <-0.7 over British Columbia).

These results are consistent with those of Davis (1976). The link between SST in the north Pacific and the overlying atmospheric circulation has become well established. The main relationship is one where the changes in the atmospheric circulation are responsible for the SST changes, as shown by simultaneous and lag correlations for instance (Davis 1976, 1978; Lanzante 1984; Wallace et al. 1990). Nevertheless, there is the strong expectation that extratropical SST anomalies also influence the atmospheric circulation. For instance, the recent SST anomaly configuration, with negative values in the central north Pacific and positive values along the west coast, exhibits the strongest persistence of any pattern during the past four decades perhaps because of the link with long-lasting atmospheric circulation anomalies (Namias et al. 1988).

Further confirmation of the link between temperatures and the atmospheric circulation comes from correlations between the NP index time series in Fig. 6 and 700 mb temperatures (Fig. 11) which reveals the four centers of the PNA. Over the Pacific and North America this pattern (with opposite sign) bears a striking resemblance to the actual surface temperature anomalies for 1977–88 (Fig. 9) including the cooling over

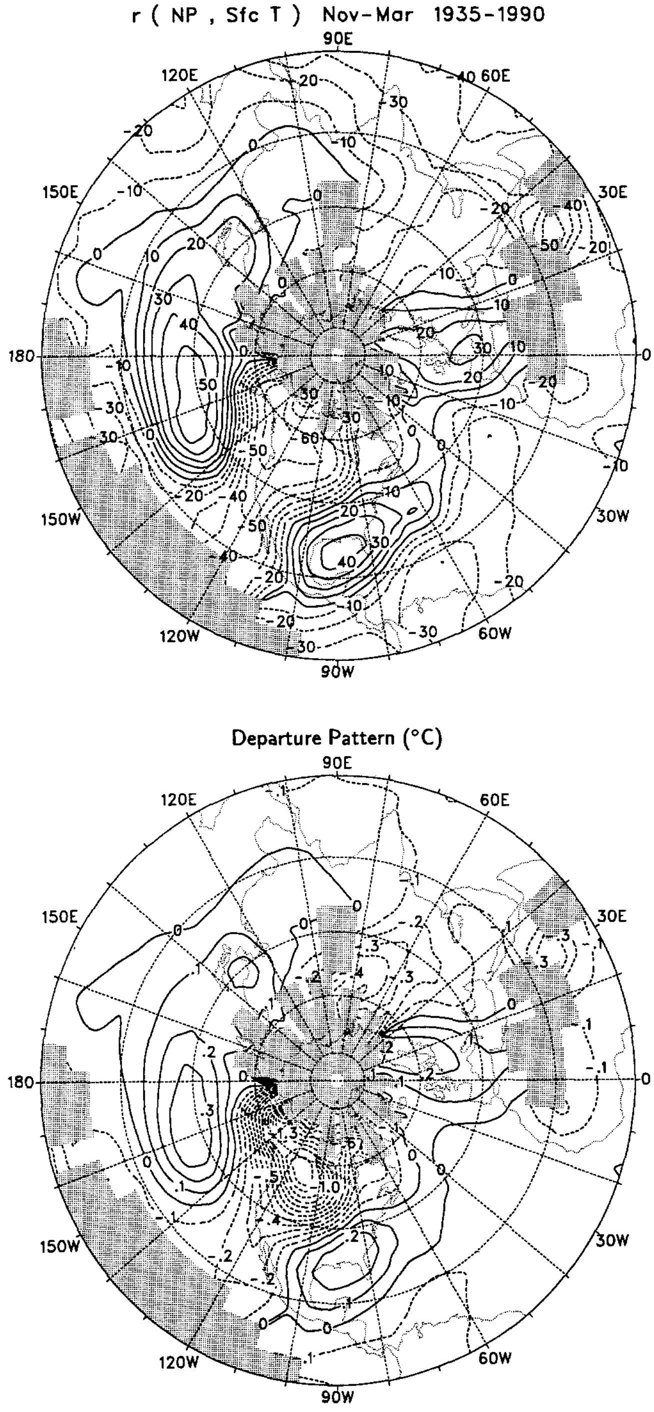

Fig. 10. Correlations (%) between the NP index and surface temperatures for 1935 to 1990 and corresponding departure pattern corresponding to a unit standard deviation of NP. Negative values are *dashed.* The 5% significance level is 0.27. *Shaded areas* indicate insufficient data

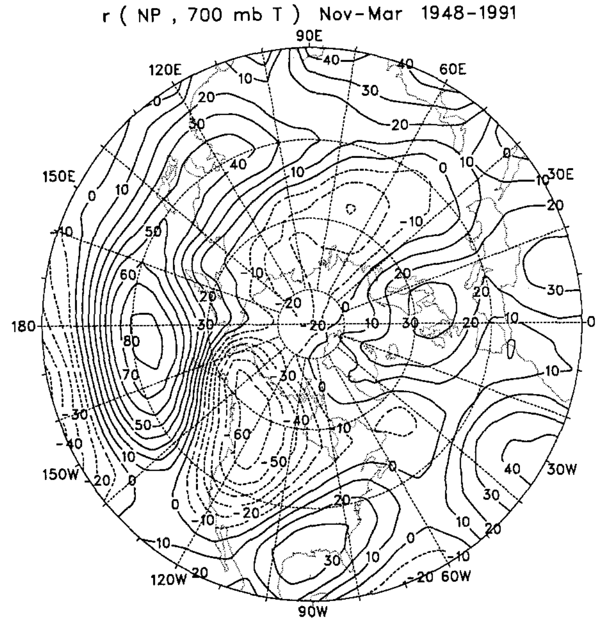

Fig. 11. Correlations (%) between the NP index in Fig. 6 and 700 mb temperatures. Negative values are *dashed.* The 5% significance level is 0.30. 20% of the variance is accounted for by the correlations over the 140°E to 60°W, 30–65°N region

the eastern part of North America. As shown in Fig. 10, the latter is thus revealed as part of the overall teleconnection pattern. Over most of the domain, the 700 mb correlations are highest at zero lag. The exception is for the center over the southeastern US, where correlations are 10% higher one month later, indicating that the development of the teleconnection downstream and the associated change in tracks of synoptic systems (e.g., Lau 1988; Rogers and Rohli 1991) may be somewhat delayed.

To complete the picture, Fig. 12 shows the correlations of the NP index with the 500 mb height field and the corresponding departure pattern. Once again, the PNA pattern emerges strongly, with all the centers in (1) showing up, although the associated anomaly departure pattern clearly emphasizes the north Pacific.

3 Changes in storm tracks and their effects on the mean flow

It is not practicable to document the exact changes in storm tracks and the effects of the changes in transient eddy heat and vorticity fluxes that occurred with the change in late 1976 because the high quality global analyses required have become available only since 1979. Accordingly, we have restricted the analysis to recent interannual variations and compared the near-normal NP with the very-low NP winters since then. Composites have been computed of a number of quantities that illustrate the changes in storm tracks and eddy fluxes, as well as the corresponding changes in outgoing longwave radiation (OLR). The composites used the following: low NP winters: 1980–81, 82–83, 83–84, 85–86, 86–87; normal NP years: 1981–82, 84–85, 88–89, 89–90, 90–91.

The eddy statistics used for this part of the study come from ECMWF analyses filtered to retain fluctuations between 2 and 8 days using the bandpass filter described by Trenberth (1991b). Figure 13 shows the "normal" transient eddy poleward heat flux $\overline{v'T'}$ at

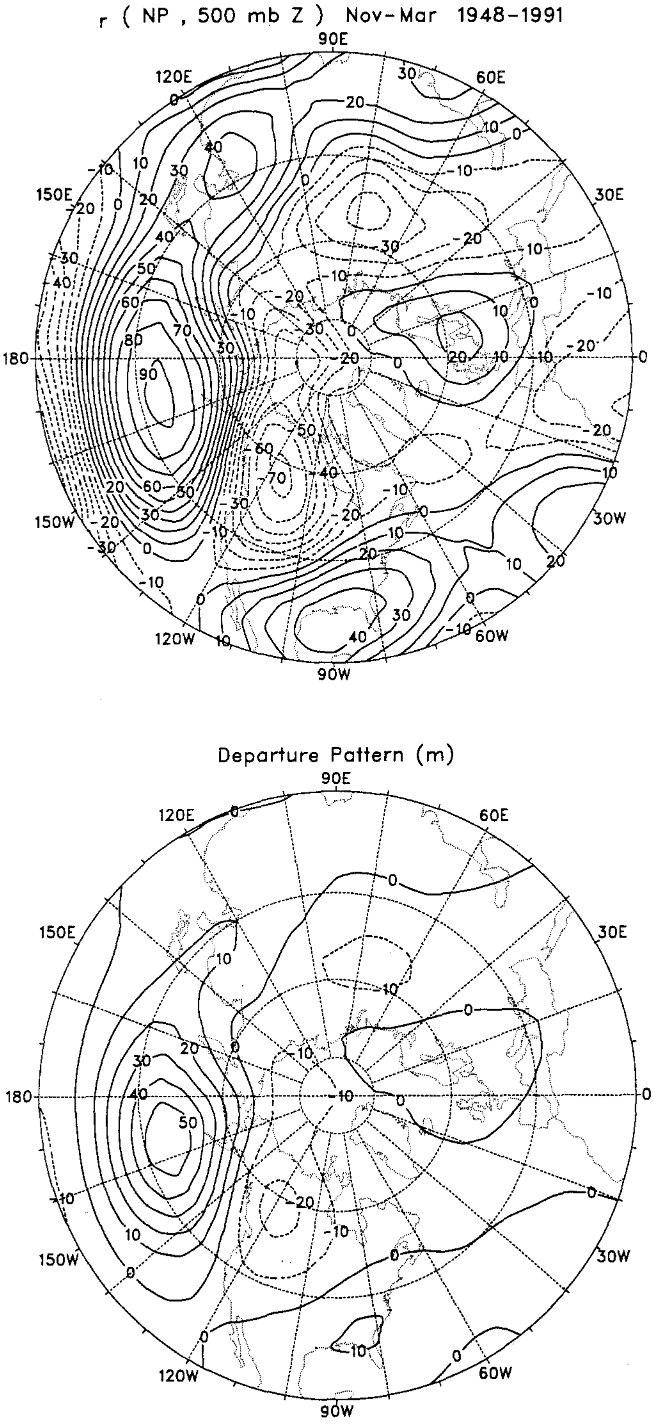

Fig. 12. Correlations (%) of the November–March NP index with 500 mb heights for 1948 to 1991 and corresponding departure pattern corresponding to a unit standard deviation of NP. Negative values are *dashed.* 26% of the variance is accounted for by the correlations over the 140°E to 60°W, 30–65°N region

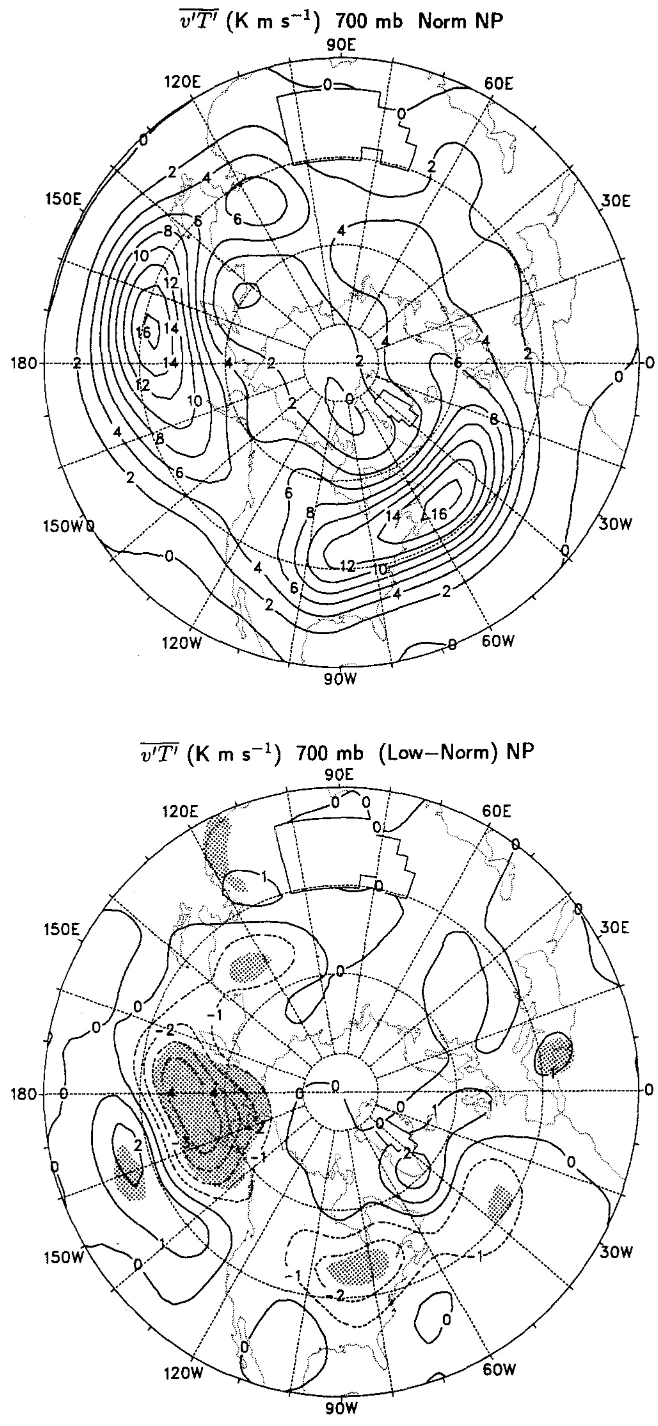

Fig. 13. Mean storm tracks for normal NP years and the anomalies, low – normal NP values, as revealed by the 700 mb transient eddy heat flux $\overline{v'T'}$ bandpassed to include 2 to 8 day period fluctuations, K m s^{-1}. Negative values are *dashed* and results are smoothed to T21 resolution. Values significantly different from zero at the 5% level using a t test are *stippled* on the *lower panel*

700 mb, where the prime indicates the filtered perturbation and the bar is both the 5 month and composite 5 year mean. Also shown in the lower panel is the difference low minus normal NP values which reveals the southward shift in the activity associated with the storm track over the north Pacific but with reduced activity extending downstream over North America. A similar pattern emerges at 850 mb. Other indicators of storm track activity (Trenberth 1991b) reveal a similar pattern; e.g., see Fig. 14 which shows $s(z) = \overline{(z'^2)}^{1/2}$, and also $s(v)$ (not shown). For $s(v)$ the dipole pattern of enhanced activity across the north Pacific south of

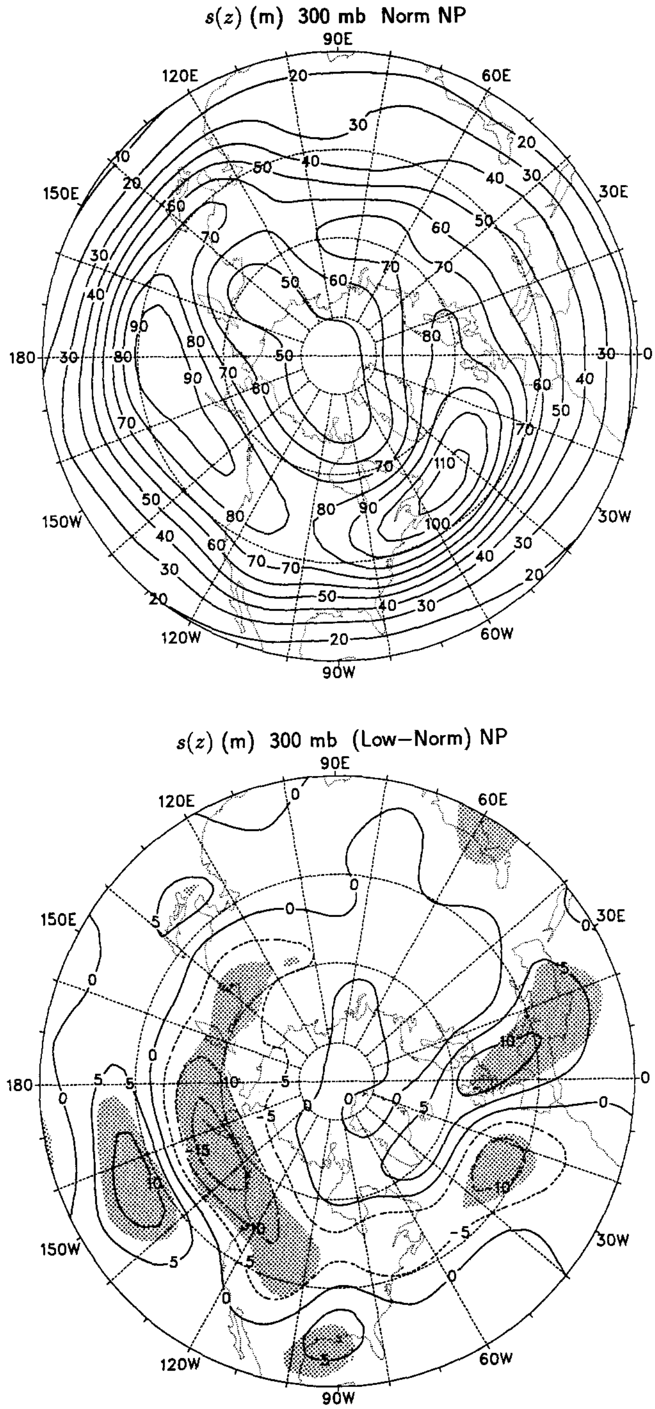

Fig. 14. Mean storm tracks for normal NP years and the anomalies, low – normal NP values, as revealed by the 300 mb root mean square transient geopotential height $s(z)$ bandpassed to include 2 to 8 day period fluctuations, m. Negative values are *dashed* and results are smoothed to T21 resolution. Values significantly different from zero at the 5% level using a t test are *stippled* on the *lower panel*

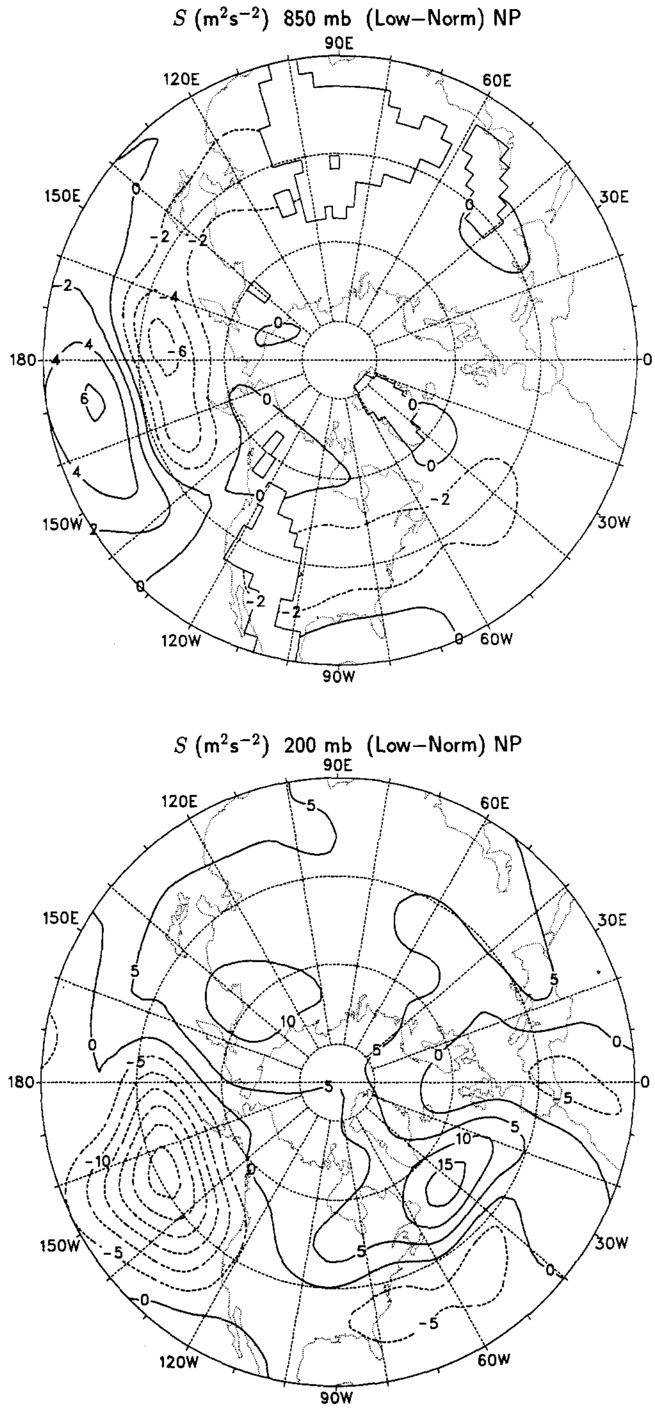

Fig. 15. Forcing of the anomalous mean stream function by the transient eddy vorticity flux $S = -\nabla^{-2}(\nabla \cdot \overline{\mathbf{v}'\zeta'})$ at 200 and 850 mb, in $m^2 s^{-2}$. Shown is the composite for the 5 low NP winters minus 5 normal NP winters (see text). Negative values are *dashed* and the results have been smoothed to T21 resolution

about 40°N and over the southern United States, and reduced activity farther north is especially pronounced. The pattern in Fig. 13 supports that found by Rogers and Raphael (1992) for composites of PNA differences.

The systematic change in the storm tracks allows the possibility that the heat and momentum or vorticity fluxes may have helped maintain the anomalous mean circulation. To pursue this possibility, we have computed localized Eliassen-Palm (E-P) fluxes following the formulation of Trenberth (1987). The eddy forcings by baroclinic (heat flux) and barotropic (momentum flux) effects on both the eastward and northward velocity components have been computed. In the upper troposphere the change in the horizontal E-P flux component is dominant and it proves easier to summarize the results by examining the eddy vorticity fluxes expressed as the tendency in maintaining the mean rotational part of the flow. Consequently, we have computed the quantity Hoskins et al. (1983) call S

$$S = -\nabla^{-2}(\nabla \cdot \overline{\mathbf{v}'\zeta'}). \quad (2)$$

S is therefore the transient eddy forcing of the mean streamfunction.

Figure 15 shows S at 850 and 200 mb for the composite low-normal NP values. At 200 mb the dominant feature is a large cyclonic circulation forcing over the north Pacific which coincides with the anomalous mean circulation. This shows that the transient eddies are systematically reinforcing and helping to maintain the upper tropospheric rotational flow in its anomalous form for a large negative NP index. Held et al. (1989) and Branstator (1992) have found similar results from linear model analyses of atmospheric general circulation model (GCM) simulations of the response to tropical heating and unforced low-frequency variability, respectively, with the transient eddy vorticity flux contributing to a strong positive feedback.

At 850 mb, and more generally in the lower troposphere, the pattern is quite different and consists of a dipole pattern that would force a cyclonic circulation over the Aleutians but with a strong anticyclonic circulation south of 40°N. The tendencies are also much smaller at 850 mb and they prove to be much smaller than the baroclinic component. Therefore, in the lower troposphere, the effects of the anomalous transient eddy heat fluxes are more important and the vorticity flux forcing is not simply acting to reinforce the anomalous flow, as it is in the upper troposphere.

The effects of the transient eddy heat flux as seen through the E-P flux are not easy to interpret. Accordingly we have found it more fruitful to examine the anomalous eddy forcing through the thermodynamic equation as the tendency in the mean temperature field

$$T_t = -\nabla \cdot \overline{\mathbf{v}'T'}. \quad (3)$$

Figure 16 shows the 700 mb perturbation mean temperature for the composited low-normal NP differences and the heat flux divergence from (3). It reveals a striking negative correlation (pattern correlation of -0.63 for the hemisphere 20–65°N) which implies that the high frequency transient eddies are acting to destroy the mean temperature perturbation in a diffusive manner on an e-folding time scale of 13.27 days[3].

This further illustrates that it is the advection by the mean flow that is offsetting the eddy forcing and maintaining the temperature perturbation. The relationship shown in Fig. 16 is compatible with the view that the transients are baroclinic eddies influenced by the anomalous temperature gradients on which they feed to produce downgradient transports (e.g., van Loon 1979). Lau (1979), Lau and Wallace (1979), and Lau

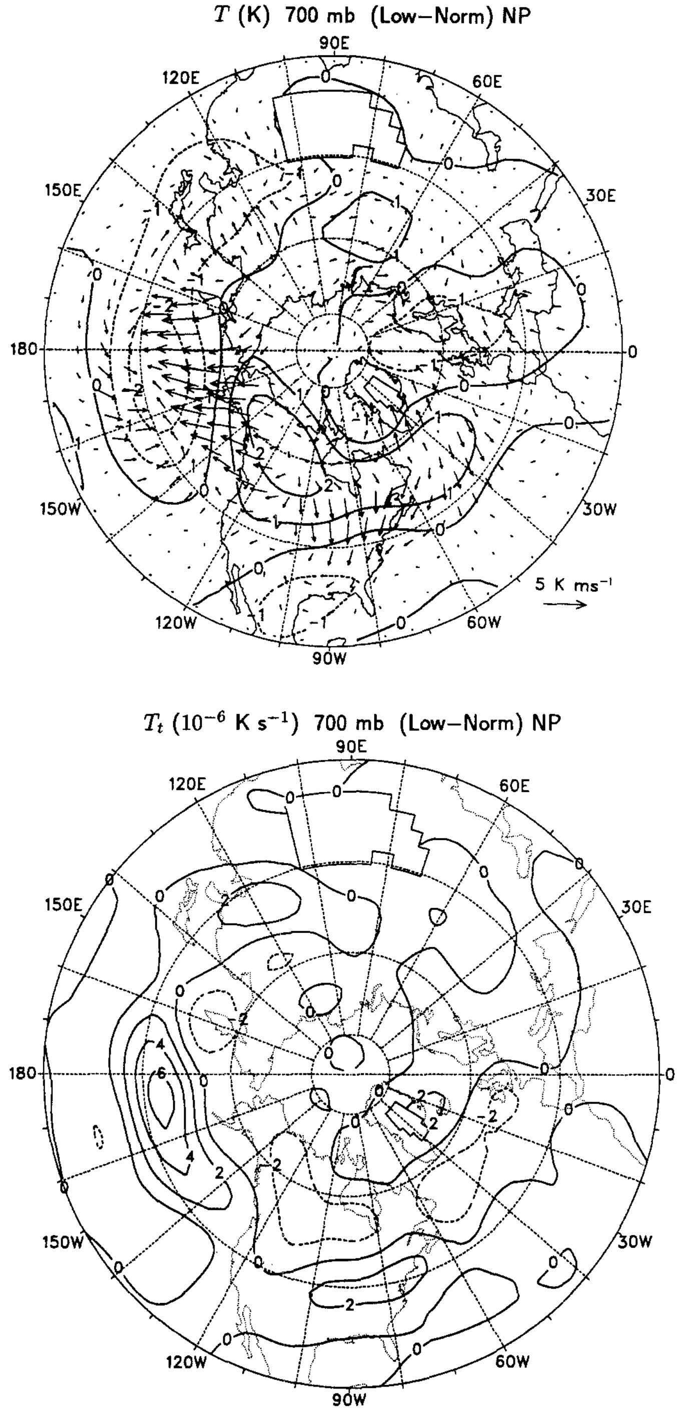

Fig. 16. The composite for the 5 low NP winters minus 5 normal NP winters (see text). Negative values are *dashed* and the results have been smoothed to T21 resolution. *Top:* mean temperature anomalies at 700 mb, K, along with the anomalous heat flux by the 2–8 day transient eddies. *Bottom:* forcing of the anomalous mean temperature by the transient eddy heat flux $T_t = -\nabla \cdot \overline{\mathbf{v}'T'}$ at 700 mb, in 10^{-6} K s^{-1}

[3] The ratio of the standard deviations of the two panels in Fig. 16 gives a time scale of 8.40 days, the 13.27 days is the result from the regression so that it includes a factor of 0.63^{-1} from the correlation coefficient

and Holopainen (1984) previously found from observations that the time mean temperature field is dissipated by the transient eddy heat fluxes, and Ting (1991) has found the same result in an idealized GCM. While Lau and Wallace (1979) note that there was no consistent relationship between the total transient eddy heat flux and the mean temperature gradient, the relationship is improved somewhat by use of only the 2–8 day period transients (Fig. 16). However, the best relationship between the transients and the mean flow is that between the divergence of the transient heat flux and the mean temperature anomaly.

Consequently, the picture emerging from the transient eddy forcing is mixed. In the lower troposphere the high frequency transients act to interfere with the anomalous mean flow while in the upper troposphere, the vorticity fluxes act to reinforce the anomalous circulation. It is clear that the change in storm tracks plays a significant role in shaping the anomalous mean pattern. Moreover, the model simulations of Held et al. (1989), Lau and Nath (1990) and Kushnir and Lau (1992) indicate that the net effect of the transient eddies is to provide a strong positive feedback in the Pacific. These reinforce the observational result of Lau and Holopainen (1984) which showed that it is the effects of the eddy vorticity fluxes which dominate in maintaining the stationary mean waves. The strong asymmetric climatological flow is an important factor in this result, as the transient eddies in an idealized zonally symmetric model climate behave quite differently and damp the response forced by tropical heating (Ting and Held 1990). The primary importance of the transient eddy forcing has also been found for observed mean anomalies during the 1982–83 ENSO event (Kok and Opsteegh 1985).

4 Causes of change in the north Pacific

Examination of the possible causes of the changes focuses attention on the association between the large-scale coherent climate variations and changes in atmospheric waves. The stationary planetary waves in the atmosphere are forced by orography and patterns of diabatic heating arising from the distribution of land and sea, both in the extratropics and in the tropics (e.g., Frankignoul 1985). Therefore, in the NH, changes in diabatic heating, for instance, can change the planetary waves and associated poleward heat fluxes. This mechanism does not operate in summer, nor does it work at any time of year in the SH where heat transports are dominated by the transient component (van Loon 1979). In addition, as seen in Section 3, by altering the temperature gradients that the transients feed on through baroclinic instability, there are changes in the transient storm tracks.

When possible causes of changes and teleconnections are considered for the North Pacific, one prospect is in situ forcing through the influence of extratropical SST anomalies in the north Pacific on the circulation (Namias 1959, 1963). It has been difficult to substantiate such influences either statistically (Davis 1976, 1978) or with models (Ting 1991; Kushnir and Lau 1992).

While the changes in eddy transports from the altered synoptic systems (Sect. 3) are one major complication, another is that the atmospheric heating effects may not be local. The sensible heat exchanged between the ocean and atmosphere is realized locally, but the latent heat lost by the ocean through evaporation is realized only as an increase in moisture, and the actual atmospheric heating is not realized until precipitation occurs, often far downstream. This latter aspect depends on the prevailing synoptic situation at the time and varies with location according to the prevailing winds and background climatological flow. These nonlocal effects are, therefore, a sensitive function of position and they add a large nondeterministic component to any forcing. This means that it is much more difficult to detect any systematic effects in both the real atmosphere and models. It also helps account for differences in results from many different model experiments, because inserted SST anomalies vary in location and intensity and the model climatologies vary. Placing "super SST anomalies" into a model will enhance the local effects so that results are more likely to appear as significant, but they are also much more likely to be unrealistic and inappropriate for the real atmosphere.

Insofar as the effects on planetary waves are concerned, enhanced land-sea contrasts would be needed to give a deeper Aleutian low, whereas the observations show the latter was mostly accompanied by below normal SSTs. In addition, changes in snow cover over Siberia appear to be capable of altering the Siberian high and Aleutian low (Yamazaki 1989).

Because of the tendency for atmospheric motions to conserve absolute vorticity, atmospheric motions occur as Rossby waves. A consequence of this is that local forcing of such waves sets up a wave train of disturbances and "teleconnections" downstream. Teleconnections are important because they induce anomalies in the circulation and associated anomalies in temperature and precipitation in remote regions. The best known examples of global impacts of local forcing are with changes in tropical SSTs such as the El Niño-Southern Oscillation (ENSO) phenomenon, whereby coupling between changes in the atmosphere and the underlying ocean in the tropical Pacific are linked by teleconnections to higher latitudes (Bjerknes 1969; Horel and Wallace 1981). The 1988 North American drought appears to have been one example of this (Trenberth et al. 1988; Trenberth and Branstator 1992).

5 Links with the tropical Pacific

The period of the deeper Aleutian low regime extends from 1976–77 to 1987–88 when there were three El Niño (warm) events in the tropical Pacific but no compensating La Niña (cold) events, so that the tropical Pacific experienced above normal SSTs and a persis-

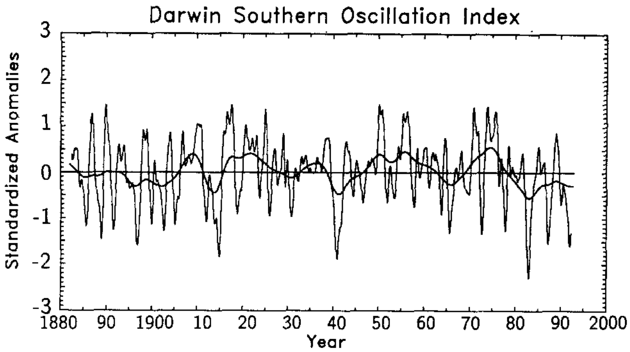

Fig. 17. Time series of the normalized Southern Oscillation Index (minus Darwin sea level pressure anomalies) monthly, filtered with an 11 term low pass filter designed to remove fluctuations less than a year (Trenberth 1984) and with a low pass spline filter that removes periods less than 10 years

tently negative Southern Oscillation index for that period (Fig. 17). Modeling studies (e.g., Blackmon et al. 1983; Alexander 1992b) confirm the causal link between SSTs in the tropics and the north Pacific circulation, with a deeper Aleutian low set up as a teleconnection due to El Niño conditions. Alexander (1992a, b) further shows that the observed changes in the north Pacific Ocean SSTs can be largely accounted for by the atmospheric changes through the associated changes in surface fluxes and mixing through the upper layers of the ocean and deepening of the mixed layer through entrainment. But the results obtained here are not simply due to the 1982–83 and 1986–87 El Niños, the Aleutian low was also much deeper than normal in several other years and especially in the winter of 1980–81. Note also from Fig. 7 that the previous time when comparably low values occurred over the north Pacific was during the major 1939 to 1942 El Niño event.

Since the late 1970s, increases in SSTs throughout the tropics of the central and eastern Pacific, as well as the Indian Ocean, have been linked to enhanced convective activity in the same region (Nitta and Yamada 1989) although this has been questioned by Chelliah and Arkin (1992). There is also emerging evidence for increased tropospheric temperatures and water vapor in the western tropial Pacific after 1976 (Hense et al. 1988; Gaffen et al. 1991). We have examined the composites from Section 3 for low versus normal NP years for OLR. Figure 18 shows that the largest changes in OLR occur in the equatorial Pacific and exceed 20 W m^{-2}, but these prove not to be statistically significant at the 95% confidence level owing to the exceptionally large OLR anomalies during the 1982–83 ENSO event. Instead it is the subtropical OLR changes that prove to be highly statistically significant, especially near Hawaii. The OLR signature that emerges as the dominant pattern is one associated with large-scale overturning, noted by Bjerknes (1969). Note that Fig. 18 relates to the interannual variability; uncertainties in OLR (Chelliah and Arkin 1992) preclude the possibility of definitely showing the changes in OLR associated with the regime that began in 1976–77.

We have examined the correlation of the NP index with the SOI for the period 1935 to 1991. The index used in Fig. 17 is minus the pressure at Darwin to form an SOI (expressed as minus Darwin to be compatible with the standard Tahiti minus Darwin index, see Trenberth 1984) as it is the most reliable homogeneous such index available (Trenberth 1984; Trenberth and Shea 1987). A low pass filter (smoothing spline fit) is shown to bring out the periods greater than ten years. For the cross correlations, however, we used the SOI as the Tahiti minus Darwin normalized surface pressure index (Trenberth 1984), but it is limited to after 1935 because the quality and completeness of the Tahiti record deteriorates prior to then. Correlations of the SOI for the combined November–March winter months with the NH sea level pressures (Trenberth and Paolino 1981) clearly reveal the link with the north Pacific and extension across North America. Highest cross correlations between SOI and NP of 0.53 occur at zero lag ± 1 month and are highly statistically significant (see Table 1).

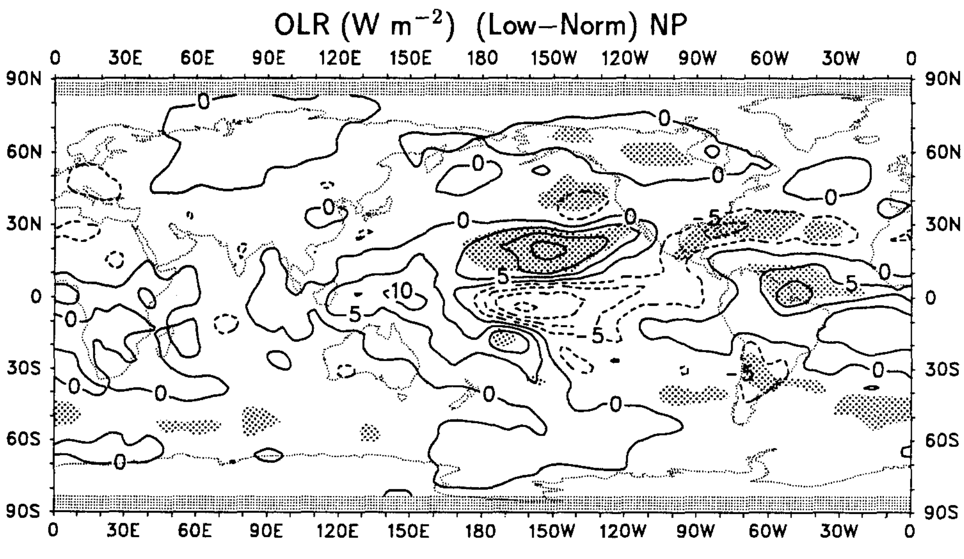

Fig. 18. Mean OLR composite anomalies for low – normal NP values in W m^{-2}. Negative values are *dashed*. The regions where values depart from zero at the 5% level of statistical significance using a *t* test are *stippled* (except at very high latitudes where the data are missing)

Table 1. Correlations (%) between the NP November–March index and indices of SST for the Niño 1+2, 3, and 4 regions and the SOI

Index Lead	Niño 1+2	Niño 3	Niño 4	Niño 3+4	SOI
+6	−39	−47	−46	−47	44
+4	−44	−49	−50	−51	46
+2	−48	−50	−49	−51	50
0	−44	−51	−45	−51	52
−2	−30	−44	−34	−43	47
−4	−18	−34	−25	−31	39
−6	−12	−15	−23	−19	16

All values are 5 month means. The period for the SOI and Niño 1+2 regions is 1935 to 1990 inclusive so that the one-tailed 1% significance level is 0.32. For the other Niño regions the period is 1951 to 1990 and the 1% significance level is 0.38. Maximum values are underlined. The lead is by the Niño SST or SOI index in months

However, this does not mean that there are not precursors in the tropics. On the contrary, it is well established that there is an evolution to the Southern Oscillation and the SST fields in the tropical Pacific as El Niño events develop (Trenberth 1976; Rasmusson and Carpenter 1981; Trenberth and Shea 1987; Wright et al. 1988). In reviewing current theories of ENSO, Philander (1992) emphasizes the "memory" of the ocean especially through changes in the heat storage. In the composite El Niño of Rasmusson and Carpenter, based on events from 1950 to 1973, the first development of SST anomalies occurs off the South American coast several months before the Southern Oscillation index responds, although the three most recent El Niño events have all evolved differently. Trenberth (1976), Trenberth and Shea (1987) and Wright et al. (1988) noted that pressures in the south Pacific (e.g., at Easter Island) respond about a season earlier than for the SOI, and Barnett (1985) suggested that changes can often be seen over the southeast Asian region before the SOI responds. Barnett et al. (1989) further suggested that this evolution may be linked to snow cover over Asia, see also Yamagata and Masumoto (1992).

We have, therefore, examined in more detail the relationships between SSTs in the tropics and the NP index. Figure 19 shows the simultaneous correlations of NP with surface temperatures over the entire region north of 35°S. This figure includes that of Fig. 10 but is on a different projection and covers a much more extensive region although for a shorter period. Problems with data coverage are severe in the tropics prior to 1951, and the treatment of the data is described in the appendix. To help summarize the results, we have computed correlations between the area-averaged SST 5-month anomalies for the tropical Pacific Niño regions (Niño 1+2 [0–10°S, 90–80°W], Niño 3 [5°N–5°S, 150–90°W] and Niño 4 [5°N–5°S, 160°E–150°W]) with NP at several leads and lags, see Table 1. As larger areas are taken, the correlation coefficient increases in magnitude, and for the Niño 3+4 regions combined, all correlations are larger with maximum values of −0.52 at 3 months lead by the SSTs. This shows that the changes in SST throughout much of the tropical Pacific lead the NP index by about three months, although the cross correlation is not sharply defined and values are only slightly smaller at zero lag. These results emphasize the involvement of the tropical SST variations in the atmospheric and surface temperature variations over the north Pacific and North America.

To summarize the results, we have compiled a tropical SST time series for the region 5°N to 10°S, 90°W to 180° (this region has much the same sign SST anomaly during ENSO events and is extensive enough to include desirable off-equatorial data). Correlations of these tropical SSTs leading the November–March NH sea level pressures by three months show the link with the north Pacific (and the NP index) and the extension across North America (Fig. 20). Note the values of opposite sign over North America which are very important as part of the overall pattern. The anomalous wind flow accompanying this pattern is indeed one where stronger southerlies along the west coast of North America accompany a negative SOI (i.e., El Niño conditions).

6 Discussion and conclusions

We updated and summarized the observed relationships involved with a decadal time scale variation in the north Pacific. A coherent pattern emerges in both the atmosphere and the ocean. The deeper Aleutian low beginning in the 1976–77 winter was accompanied by distinctive surface and tropospheric temperature

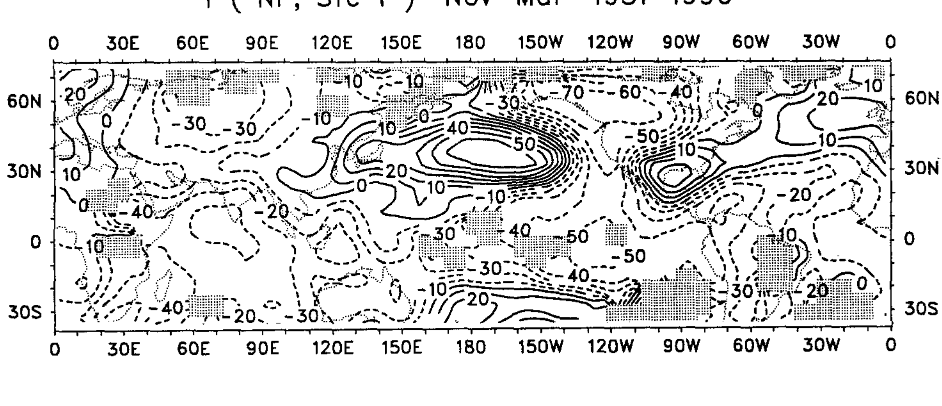

Fig. 19. Correlations (%) of the five month mean November–March NP index with surface termperatures at zero lag for 1951–1990. Negative values are *dashed* and areas of insufficient data (see appendix) are *stippled*

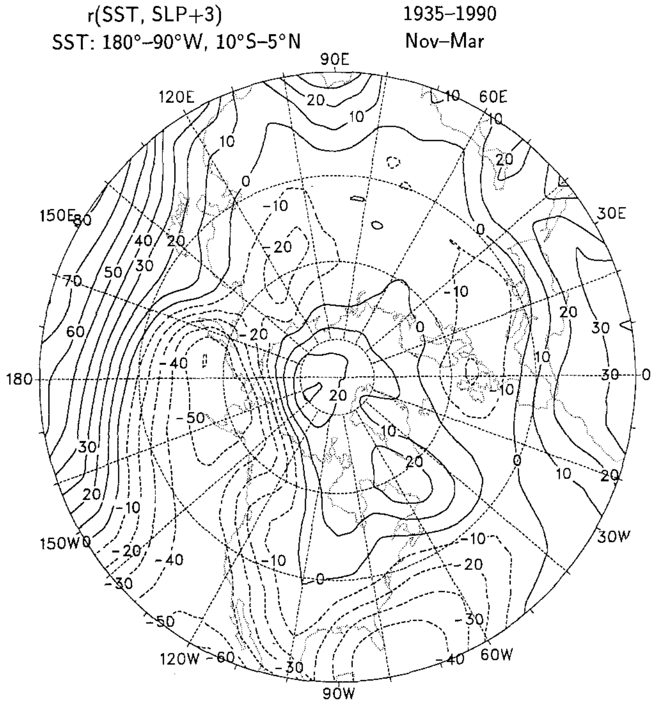

Fig. 20. Correlations of the five month mean SSTs in the region 5°N to 10°S, 90°W to 180° for August through December with November through March sea level pressures over the Northern Hemisphere for 1935 to 1990 (i.e., the tropical SSTs lead by three months). The 1% significance level is 0.34

changes that are consistent with advection by the anomalous flow, and by changes in storm tracks, coastal rainfall and surface fluxes. The corresponding changes in atmospheric eddy heat and vorticity fluxes were shown to be strongly related to the anomalous mean flow, with the heat fluxes acting in a dissipative manner but with the vorticity fluxes acting as a strong positive feedback in reinforcing the anomalous flow. It appears that the latter influence is dominant. We have also shown that there are strong teleconnections present linking the changes over the Pacific to profound changes over North America, but also with strong links to the tropics where there is good evidence of precursor changes.

On short time scales, the results reveal that the atmosphere drives the ocean with changes in SSTs occurring one to two months later, apparently because of the changes in surface sensible and latent heat fluxes combined with mixing in the ocean and entrainment (see Frankignoul 1985; Wallace et al. 1990; Lau and Nath 1990; Alexander 1992a). Nevertheless, the atmospheric influence depends greatly on the synoptic situation, so that it takes many months to sort out the signal. On a longer time scale, the coherent nature of the atmospheric and oceanic variations is highly suggestive, but the picture emerging from the empirical and modeling studies is not yet fully clear. The evidence suggests the following hypothesis.

In the tropics, coupled ocean-atmosphere interactions result in coupled modes of which ENSO is the most prominent. This results in large interannual variability in the Pacific sector with preferred time scales of 2 to 7 years, but with small amplitude decadal variations. All these fluctuations have manifestations in higher latitudes through teleconnections within the atmosphere. In the north Pacific, ENSO variability is found in the PNA pattern (and the NP index) but is best seen when averages can be taken over the entire winter half year as the noise level associated with natural weather variability is high on monthly time scales. The deepened Aleutian low in ENSO events results in a characteristic SST anomaly pattern that, on average, is enhanced through positive feedback effects from (1) effects of the extratropical SST anomaly itself, and (2) changes in momentum (and vorticity) fluxes associated with changes in high frequency storm tracks. The same influences are present on decadal time scales, but whereas the changes in SST arising from surface fluxes and mixed layer processes are dominant on interannual time scales, changes in ocean currents must also become a factor and reinforce the SST changes. Moreover, the long time scale involved in changing the currents and the Sverdrup circulation adds further persistence to the extratropical system that, along with the heat storage in the upper 500 m of the ocean, evidently serves to emphasize the decadal over interannual time scales relative to the tropics.

The system described is one where chaos (weather noise) is a prominent factor in the extratropics but the climate is moulded by the tropical influences with the ocean selectively bringing out the long time scales. The ocean is never in equilibrium. Preferred SST anomaly patterns emerge because they help reinforce the atmospheric circulation patterns rather than destroying them, as is more commonly the case.

Aspects of this hypothesis have appeared in the extensive works of Namias but here we have emphasized much more the links with the tropics. Because of climate change associated with the greenhouse gas increases, teleconnections from the tropics are apt to change as the zonal mean flow changes (Meehl et al. 1993). Also a major, but as yet unanswered question, is whether either the intensity or frequency of ENSO events might change as a result of global warming. Figure 17 reveals that the frequency and intensity of ENSO events have changed in the past (Trenberth and Shea 1987), with strong ENSO fluctuations from about 1880 to 1920, which led to the discovery and naming of the Southern Oscillation by Sir Gilbert Walker. Aside from the major event from 1939 to 1942, stronger and more regular ENSO events only resumed in the 1950s. However, the low pass curve in Fig. 17 indicates that the recent imbalance between the occurrence of warm versus cold events in the tropical Pacific is unprecedented. Alternatively, the more recent interannual variability is occurring about a different base state.

Whether the unusual 1976–1988 imbalance can be ascribed to any cause, or is merely a part of natural variability is a very difficult question to answer. The major change that occurred in March–April 1988, with a transition from El Niño to a very strong La Niña (Fig. 17, and Trenberth et al. 1989), apparently ended the climate regime although the underlying ocean currents and heat storage must be still perturbed and the pattern could reemerge. Indeed, the recent 1991–92 ENSO event was noted for exceptionally warm water along the west coast of both North and South America in early 1992.

Appendix

The manner in which missing data are handled can be important, especially when dealing with data sets with vast poorly sampled areas. Although somewhat arbitrary, the guidelines used in this study were as follows. For each gridpoint, "seasonal" values were computed only when data existed for at least 3 of the 5 months defining the season. Correlations between variables were not computed if the two variables had fewer than 75% of the total number of seasons in common. When area-averaged fields were calculated, at least 50% of the gridpoints in the area had to be sampled.

These criteria are easily met by most of the data sets used in this study. The exception is the IPCC surface temperature data set. Large areas of the tropical and Southern Hemisphere oceans are poorly sampled (e.g., Trenberth et al. 1992), and these regions have been excluded from the computations (see Fig. 19). Of the Niño regions defined in Table 1, only the Niño 1+2 region is well-defined back to 1935, and even from 1951 through 1990 the Niño 4 region is poorly sampled.

Acknowledgements. We wish to specially thank Dennis Shea for preparing some of the figures. This research is partially sponsored by the Tropical Oceans Global Atmosphere Project Office under grant NA87AANRG0208.

References

Alexander M (1992a) Midlatitude atmosphere-ocean interaction during El Niño. I. The North Pacific Ocean. J Clim 5:944–958

Alexander M (1992b) Midlatitude atmosphere-ocean interaction during El Niño. II. The Northern Hemisphere atmosphere. J Clim 5:959–972

Bakun A (1990) Global climate change and intensification of coastal ocean upwelling. Science 247:198–201

Barnett TP (1985) Variations in near global sea level pressure. J Atmos Sci 42:478–501

Barnett TP, Dümenil K, Schlese U, Roeckner E, Latif M (1989) The effect of Eurasian snow cover on regional and global climate variations. J Atmos Sci 46:661–685

Bjerknes J (1969) Atmospheric teleconnections from the equatorial Pacific. Mon Weather Rev 97:163–172

Blackmon ML, Geisler JE, Pitcher EJ (1983) A general circulation model study of January climate anomaly patterns associated with interannual variation of equatorial Pacific sea surface temperatures. J Atmos Sci 40:1410–1425

Bottomley M, Folland CK, Hsiung J, Newell RE, Parker DE (1990) Global ocean surface temperature atlas. The UK Meteorological Office

Branstator G (1987) A striking example of the atmosphere's leading traveling mode. J Atmos Sci 44:2310–2323

Branstator G (1992) The maintenance of low-frequency atmospheric anomalies. J Atmos Sci 49:1924–1945

Cayan DR (1992) Latent and sensible heat flux anomalies over the northern oceans: the connection to monthly atmospheric circulation. J Clim 5:354–369

Cayan DR, Peterson DH (1989) The influence of north Pacific atmospheric circulation on streamflow in the West. Geophys Monogr 55, Am Geophys Union 375–397

Chelliah M, Arkin P (1992) Large-scale variability of monthly outgoing longwave radiation anomalies over the global tropics. J Clim 5:371–389

Davis R (1976) Predictability of sea surface temperature and sea level pressure anomalies over the north Pacific Ocean. J Phys Oceanogr 6:249–266

Davis R (1978) Predictability of sea-level pressure anomalies over the north Pacific Ocean. J Phys Oceanogr 8:233–246

Dickson RR, Namias J (1976) North American influences on the circulation and climate of the North American sector. Mon Weather Rev 104:1255–1265

Douglas AV, Cayan DR, Namias J (1982) Large-scale changes in north Pacific and North American weather patterns in recent decades. Mon Weather Rev 112:1851–1862

Dowton MW, Miller KA (1993) The freeze risk to Florida citrus. II: Temperature variability and circulation patterns. J Clim 6:364–372

Ebbesmeyer C, Cayan DR, McLain DR, Nichols FH, Peterson DH, Redmond KT (1991) 1976 step in the Pacific climate: forty environmental changes between (1968–1975 and 1977–1984). In: Betancourt JL, Sharp VL (eds) Proc. Seventh Ann. Pacific Climate (PACLIM) Wkshp, April (1990). California Department of Water Resources Interagency Ecological Studies Program Tech. Rep. 26. 129–141

Frankignoul C (1985) Sea surface temperature anomalies, planetary waves, and air-sea feed-backs in middle latitudes. Rev Geophys 8:233–246

Gaffen DJ, Barnett TP, Elliott WP (1991) Space and time scales of global tropospheric moisture. J Clim 4:989–1008

Hamilton K (1987) Interannual environmental variation and North American fisheries. Bull Am Meteorol Soc 68:1541–1548

Held IM, Lyons SW, Nigam S (1989) Transients and the extratropical response to El Niño. J Atmos Sci 46:163–174

Hellerman S, Rosenstein M (1983) Normal monthly wind stress over the world ocean with error estimates. J Phys Oceanogr 17:1093–1104

Hense A, Krahe P, Flohn H (1988) Recent fluctuations of tropospheric temperature and water vapour content in the tropics. Meteorol Atmos Phys 38:215–227

Horel JD, Wallace JM (1981) Planetary-scale atmospheric phenomena associated with the Southern Oscillation. Mon Weather Rev 109:813–829

Hoskins BJ, James IN, White GH (1983) The shape, propagation and mean-flow interaction of large-scale weather systems. J Atmos Sci 40:1595–1612

IPCC (1990) Scientific assessment of climate change. IPCC WG I, WMO, UNEP. Houghton JT, Jenkins GJ, Ephraums JJ (eds) Cambridge U Press, Cambridge, UK

IPCC (1992) Climate Change (1992) Houghton JT, Callander BA, Varney SK (eds) Cambridge U Press, Cambridge, UK

Jones PD (1988) Hemispheric surface air temperature variations: recent trends and an up-date to 1987. J Clim 1:654–660

Kok CJ, Opsteegh JD (1985) Possible causes of anomalies in seasonal mean circulation patterns during the 1982–83 El Niño event. J Atmos Sci 42:677–694

Kushnir Y (1987) Retrograding winter time low-frequency disturbances over the north Pacific Ocean. J Atmos Sci 44:2727–2742

Kushnir Y, Lau NC (1992) The general circulation model response to a north Pacific SST anomaly: dependence on time scale and pattern polarity. J Clim 5:271–283

Lanzante JR (1984) A rotated eigenanalysis of the correlation between 700-mb heights and sea surface temperatures in the Pacific and Atlantic. Mon Weather Rev 112:2270–2280

Lau N-C (1979) The observed structure of tropospheric stationary waves and the local balances of vorticity and heat. J Atmos Sci 36:996–1016

Lau N-C (1988) Variability of the observed midlatitude storm tracks in relation to low frequency changes in the circulation pattern. J Atmos Sci 45:2718–2743

Lau N-C, Holopainen EO (1984) Transient eddy forcing of the time mean flow as identified by geopotential tendencies. J Atmos Sci 41:313–328

Lau N-C, Nath MJ (1990) A general circulation model study of the atmospheric response to extratropical SST anomalies observed in 1950–79. J Clim 3:965–989

Lau N-C, Wallace JM (1979) On the distribution of horizontal transports by transient eddies in the Northern Hemisphere winter time circulation. J Atmos Sci 36:1844–1861

Leathers DJ, Palecki MA (1992) The Pacific/North American teleconnection pattern and United States climate. II: Temporal characteristics and index specification. J Clim 5:707–716

Madden RA, Speth P (1989) The average behavior of large-scale westward traveling disturbances evident in the Northern Hemisphere geopotential heights. J Atmos Sci 46:3225–3239

Manak DK, Mysak LA (1987) Climatic atlas of arctic sea ice extent and anomalies 1953–1984. Climate Research Group Report 87–8

McFarlane GA, Beamish RJ (1992) Climatic influence linking Copepod production with strong year-classes in sablefish, Anoplopoma fimbria. Can J Fish Aquat Sci 49:743–753

Meehl GA, Branstator GW, Washington WM (1993) Tropical Pacific interannual variability and CO_2 climate change. J Clim 6:42–63

Mysak LA (1986) El Niño, interannual variability and fisheries in the northeast Pacific Ocean. Can J Fish Aquat Sci 43:464–497

Namias J (1959) Recent seasonal interactions between north Pacific waters and the overlying atmospheric circulation. J Geophys Res 64:631–646

Namias J (1963) Large-scale air-sea interactions over the north Pacific from summer (1962) through the subsequent winter. J Geophys Res 68:6171–6186

Namias J (1969) Seasonal interactions between the north Pacific Ocean and the atmosphere during the 1960s. Mon Weather Rev 97:173–192

Namias J, Yuan X, Cayan DR (1988) Persistence of north Pacific sea surface temperature and atmospheric flow patterns. J Clim 1:682–703

Nitta T, Yamada S (1989) Recent warming of tropical sea surface temperature and its relationship to the Northern Hemisphere circulation. J Meteorol Soc Japan 67:375–383

Philander SGH (1992) Ocean-atmosphere interactions in the tropics: A review of recent theories and models. J Appl Meteorol 31:938–945

Rasmusson EM, Carpenter TH (1982) Variations in tropical sea surface temperature and surface wind fields associated with the Southern Oscillation/El Niño. Mon Weather Rev 110:354–384

Rogers JC, Rohli RV (1991) Florida citrus freezes and polar anticyclones in the Great Plains. J Clim 4:1103–1113

Rogers JC, Raphael MN (1992) Meridional eddy sensible heat fluxes in the extremes of the Pacific/North American teleconnection pattern. J Clim 5:127–139

Royer TC (1989) Upper ocean temperature variability in the northeast Pacific Ocean: is it an indicator of global warming? J Geophys Res 94:18175–18183

Salmon DK (1992) On interannual variability and climate change in the north Pacific. Ph D Thesis. Univ of Alaska, USA

Sekine Y (1988) Anomalous intrusion of the Oyashio east of Japan. I. Influence of the interannual and seasonal variations in the wind stress over the north Pacific. J Geophys Res 93:2247–2255

Ting M (1991) The stationary wave response to a midlatitude SST anomaly in an idealized GCM. J Atmos Sci 48:1249–1275

Ting M, Held IM (1990) The stationary wave response to a tropical SST anomaly in an idealized GCM. J Atmos Sci 47:2546–2566

Trenberth KE (1976) Spatial and temporal variations of the Southern Oscillation. Q J R Meteorol Soc 12:639–653

Trenberth KE (1984) Signal versus noise in the Southern Oscillation. Mon Weather Rev 112:326–332

Trenberth KE (1987) The role of eddies in maintaining the westerlies in the Southern Hemisphere winter. J Atmos Sci 44:1498–1508

Trenberth KE (1990) Recent observed interdecadal climate changes in the Northern Hemisphere. Bull Am Meteorol Soc 71:988–993

Trenberth KE (1991a) Recent climate changes in the Northern Hemisphere. DOE Workshop, 8–12 May (1989, Amherst, Mass. In: Schlesinger M (ed) Greenhouse-gas-induced climate change: a critical appraisal of simulations and observations. Elsevier, Amsterdam, pp 377–390

Trenberth KE (1991b) Storm tracks in the Southern Hemisphere. J Atmos Sci 48:2159–2178

Trenberth KE, Branstator GW (1992) Issues in establishing causes of the 1988 drought over North America. J Clim 5:159–172

Trenberth KE, Paolino DA (1980) The Northern Hemisphere sea-level pressure data set: Trends, errors, and discontinuities. Mon Weather Rev 108:855–872

Trenberth KE, Paolino DA (1981) Characteristic patterns of variability of sea level pressure in the Northern Hemisphere. Mon Weather Rev 109:1169–1189

Trenberth KE, Shea DJ (1987) On the evolution of the Southern Oscillation. Mon Weather Rev 115:3078–3096

Trenberth KE, Branstator GW, Arkin PA (1988) Origins of the 1988 North American drought. Science 242:1640–1645

Trenberth KE, Olson JG, Large WG (1989) A global ocean wind stress climatology based on ECMWF analyses. NCAR Tech Note NCAR/TN-338+STR

Trenberth KE, Christy JR, Hurrell JW (1992) Monitoring global monthly mean surface temperatures. J Clim 5:1406–1423

van Loon H (1979) The association between latitudinal temperature gradient and eddy transport. I: Transport of sensible heat in winter. Mon Weather Rev 107:525–534

Venrick EL, McGowan JA, Cayan DA, Hayward TL (1987) Climate and chlorophyll a: long-term trends in the central north Pacific Ocean. Science 238:70–72

Wallace JM, Gutzler DS (1981) Teleconnections in the geopotential height field during the Northern Hemisphere winter. Mon Weather Rev 109:784–812

Wallace JM, Smith C, Jiang Q (1990) Spatial patterns of atmosphere-ocean interaction in the northern winter. J Clim 3:990–998

Wright PB, Wallace JM, Mitchell TP, Deser C (1988) Correlation structure of the El Niño/Southern Oscillation phenomenon. J Clim 1:609–625

Yamagata T, Masumoto Y (1992) Interdecadal natural climate variability in the western Pacific and its implication in global warming. J Meteorol Soc Japan 70:167–175

Yamazaki K (1989) A study of the impact of soil moisture and surface albedo changes on global climate using the MRI GCM-I. J Meteorol Soc Japan 67:123–146